Environmental Toxicology and Pharmacology 104 (2023) 104285

Contents lists available at ScienceDirect

Environmental Toxicology and Pharmacology

journal homepage: www.elsevier.com/locate/etap

Role of voltage-dependent calcium channels on the striatal in vivo dopamine release induced by the organophosphorus pesticide glyphosate

Carmen Costas-Ferreira [a], Ana Carolina de Jesus Silva [b], Lorane Izabel da Silva Hage-Melim [b], Lilian R. Ferreira Faro [a,*]

[a] Department of Functional Biology and Health sciences, Faculty of Biology, University of Vigo, Spain
[b] Laboratory of Pharmaceutical and Medicinal Chemistry, Federal University of Amapá, Macapá, Brazil

ARTICLE INFO

Edited by Dr. M.D. Coleman

Keywords:
Glyphosate
Voltage-sensitive calcium channels
in vivo dopamine release
Cerebral microdialysis
Molecular docking

ABSTRACT

In the present study, we investigated the role of voltage-sensitive calcium channels (VSCCs) on the striatal dopamine release induced by the pesticide glyphosate (GLY) using selective VSCC inhibitors. The dopamine levels were measured by in vivo cerebral microdialysis coupled to HPLC-ED. Nicardipine (L-type VSCC antagonist) or ω-conotoxin MVIIC (non-selective P/Q-type antagonist) had no effect on dopamine release induced by 5 mM GLY. In contrast, flunarizine (T-type antagonist) or ω-conotoxin GVIA (neuronal N-type antagonist) significantly reduced GLY-stimulated dopamine release. These results suggest that GLY-induced dopamine release depends on extracellular calcium and its influx through the T- and N-type VSCCs. These findings were corroborated by molecular docking, which allowed us to establish a correlation between the effect of GLY on blocked VSCC with the observed dopamine release. We propose new molecular targets of GLY in the dorsal striatum, which could have important implications for the assessment of pesticide risks in non-target organisms.

1. Introduction

Glyphosate (GLY) is a widely used herbicide whose supposed low toxicity has been questioned in recent years, as exposure to this compound has recently been linked to the development of a wide range of neurotoxic effects. One of the effects reported in several studies was motor impairment in animals exposed to GLY, which has been associated with severe alterations in dopaminergic neurotransmission both in vitro (Faria et al., 2021; Martínez et al., 2018) and in vivo (Costas-Ferreira et al., 2023; Faro et al., 2022; Hernández-Plata et al., 2015). However, these data seem contradictory, as they show that the pesticide was able to induce both increases (Costas-Ferreira et al., 2023; Faria et al., 2021; Faro et al., 2022) and decreases (Hernández-Plata et al., 2015; Martínez et al., 2018) in striatal dopamine levels.

In a previous and more comprehensive study from our laboratory, it was demonstrated that systemic or intrastriatal administration of GLY induced dose-dependent increases in dopamine release from dorsal striatum in awake and freely moving animals. According to these data, GLY could increase extracellular levels of dopamine both by increasing its exocytotic release and through an action on the dopamine transporter (Costas-Ferreira et al., 2023).

Exocytotic release of neurotransmitters depends on calcium (Ca^{2+}) entry into neurons through voltage-sensitive calcium channels (VSCCs). VSCCs are transmembrane proteins that, based on their electrophysiological and pharmacological properties, are usually classified into low-voltage-activated channels (T-type) and high-voltage-activated channels (L-, N- and P/Q-types) (Zamponi et al., 2015). All of them show different location depending on their properties and functions. In the substantia nigra (*pars compacta*) and striatum, L-, N-, and P/Q-type VSCCs have been identified, and N-type and P/Q-type VSCCs seem to play a predominant role in dopamine release (Bergquist et al., 1998; Turner et al., 1993).

Abbreviations: Ca^{2+}, calcium; $Cav_{1.3}$, L-type VSCC; $Cav_{2.2}$, N-type VSCC; $Cav_{3.3}$, low-voltage activated T-type VSCC; CNS, central nervous system; DOPAC, 3,4-dihydroxyphenylacetic acid; FLU, flunarizine; GLY, glyphosate; HPLC-EC, high-performance liquid chromatography with electrochemical detection; HVA, homovanillic acid; nAChR, nicotinic acetylcholine receptors; NIC, nicardipine; NMDAR, N-methyl-D-aspartate receptor; PDB, Protein Data Bank; PMZ, pimozide; RM1, Recife model 1; RMSD, root mean square derivation; VSCC, voltage-sensitive calcium channel; ω-conotox GVIA, ω-conotoxin GVIA; ω-conotox MVIIC, ω-conotoxin MVIIC.

* Correspondence to: Department of Functional Biology and Health Sciences, Faculty of Biology, University of Vigo, Campus Lagoas-Marcosende, 36310 Vigo, Spain.

E-mail address: lilianfaro@uvigo.gal (L.R.F. Faro).

https://doi.org/10.1016/j.etap.2023.104285
Received 10 July 2023; Received in revised form 25 September 2023; Accepted 29 September 2023
Available online 30 September 2023

Therefore, the main objective of the present study is to investigate the role of extracellular Ca^{2+} and VSCCs of T-, L-, N-, and P/Q-type on the GLY-induced in vivo dopamine release from rat dorsal striatum. For this we use flunarizine (FLU), nicardipine (NIC), ω-conotoxin MVIIC (ω-conotox MVIIC), and ω-conotoxin GVIA (ω-conotox GVIA) as selective antagonists of T-, L-, N-, and P/Q-type channels, respectively. Additionally, we use molecular docking to evaluate the interaction of the GLY and the different ligands with the VSCCs in order to establish a possible correlation between the effect of the pesticide on the blocked VSCC with the dopamine release observed by brain microdialysis.

2. Material and methods

2.1. Animals

Adult female Sprague-Dawley rats (250–350 g) obtained from the Breeding Facility of the CINBIO (*Centro de Investigaciones Biomédicas*) of the University of Vigo (Spain) were used in all experiments. The animals were housed in standard cages and kept under constant humidity and temperature conditions (22 ± 2 °C) with controlled periods of light-darkness (14 and 10 h, respectively). Animals had free access to commercial food and tap water, which were available ad libitum. All experiments were carried out in accordance with the Guidelines of the European Union Council 2010/63/EU and the Spanish State (*Real Decreto* 53/2013) for the use of laboratory animals, and with the authorization of the "Ethics Committee on Animal Welfare" of the University of Vigo (ES360570215601/21/FUN01/BIOL.AN.08/LFF/01). Every effort was made to avoid animal suffering and distress.

The present study was carried out with female rats. The use of female rats is supported by previous data showing that no sex differences have been found in the variability of behavioral, electrophysiological, neurochemical, or histological measurements (Becker et al., 2016; Egenrieder et al., 2020). Besides, previous data from our laboratory did not show significant differences between males and females both in baseline dopamine levels and in the effects produced by different types of drugs, toxic, or toxins (Arias et al., 1998; Alfonso et al., 2019; Campos et al., 2007; Faro et al., 2022).

2.2. Drugs and treatment

GLY (98% purity) was obtained from Pestanal® (Sigma-Aldrich, Germany). Dopamine, 3,4-dihydroxyphenylacetic acid (DOPAC), homovanillic acid (HVA), FLU and NIC, were obtained from Sigma-Aldrich (St. Louis, USA). The ω-conotox MVIIC was purchased from Abcam plc (Cambridge, UK) and the ω-conotox GVIA was purchased from Tocris (Bristol, UK). All other chemicals and reagents were of analytical grade. The water used for the preparation of reagents, solvents and chromatographic solutions was obtained from a MilliQ system (Millipore).

The GLY concentration (5 mM) and the time of administration (60 min) are the same used in previous studies of our laboratory to study the mechanisms of action of the pesticide (Costas-Ferreira et al., 2023; Faro et al., 2022). The VSCC antagonist concentrations are consistent with those used in previous reports using brain microdialysis technique (Bergquist et al., 1998; Burley and Dolphin, 2000; El Ayadi et al., 2001; Faro et al., 2018, 2022; Furukawa et al., 1999; Kato et al., 1992; Lohr et al., 2005; Rocchitta et al., 2004; Thaler et al., 2001; Ye et al., 2011).

A total of 57 animals were used in the present study, which were divided into the ten experimental groups described in Table 1. Both GLY and antagonists were dissolved in perfusion medium and infused locally into the dorsal striatum through a microdialysis probe.

2.3. Microdialysis procedure

For microdialysis sampling, the animals were anesthetized with chloral hydrate (400 mg/kg i.p.) and placed in a stereotactic device (Nashigire SR-6, Japan). An incision was made in the skin located at the top of the skull and a small hole was drilled in the exposed skull surface according to the following coordinates established by the atlas of Paxinos and Watson (1998): A/P + 1,00 mm; L+ 3,00 mm; V+ 6,00 mm; taking the Bregma as a point of reference. This location corresponds to the left dorsal striatum, where a CMA12 guide cannula (CMA/Microdialysis, Sweden) was implanted.

Twenty-four hours after implantation of the guide cannula and just before the start of the experiments, a CMA12 microdialysis probe (0.5 mm diameter, membrane length 3 mm) (CMA/Microdialysis, Sweden) was inserted into the striatum through the guide cannula. The probe was connected to a microdialysis pump (CMA/402, CMA/Microdialysis, Sweden) and infused with a Ringer's solution (147 mM NaCl, 4 mM KCl and 2.4 mM CaCl2, pH = 7.4) at a constant flow rate of 1.5 μL/min.

Samples were collected every 20 min in all experiments performed. In the first group of experiments, after collecting three basal samples (60 min), GLY was infused for 60 min; after this, the medium was then switched back to the unmodified Ringer's solution and sampling was continued for an additional period of 60 min. For the studies of the role of Ca^{2+} in the GLY-induced dopamine release, after collecting three basal samples, a Ringer's solution without Ca^{2+} (149.4 mM NaCl, 4 mM KCl, pH = 7.4) was infused for 60 min followed by administration of GLY dissolved in this Ringer without Ca^{2+} (60 min); finally, unmodified Ringer's solution was perfused for the remaining 60 min of the experiment. In the last group of experiments, carried out to study the effects of VSCC antagonists, after collecting three basal samples, the different antagonists were infused for 60 min and then together with GLY, which was infused throughout the third hour of the experiment. Next, the medium was switched back to the unmodified Ringer's solution and sampling was continued for an additional period of 60 min

Table 1
Experimental groups used in the microdialysis experiments.

Group	Treatment	Experimental design			
		60 min (3 samples)	60 min (3 samples)	60 min (3 samples)	60 min (3 samples)
1	GLY 5 mM (n = 9)	RINGER	GLY 5 mM	RINGER	-
2	GLY + Ca^{2+}-free Ringer (n = 5)	RINGER	Ca^{2+}-free Ringer	GLY 5 mM + Ca^{2+}-free Ringer	RINGER
3	GLY + FLU (n = 5)	RINGER	FLU 10 μM	GLY 5 mM + FLU 10 μM	RINGER
4	GLY + FLU (n = 5)	RINGER	FLU 100 μM	GLY 5 mM + FLU 100 μM	RINGER
5	GLY + NIC (n = 5)	RINGER	NIC 10 μM	GLY 5 mM + NIC 10 μM	RINGER
6	GLY + NIC (n = 8)	RINGER	NIC 100 μM	GLY 5 mM + NIC 100 μM	RINGER
7	GLY + ω-contox MVIIC (n = 5)	RINGER	ω-contox MVIIC 20 μM	GLY 5 mM + ω-contox MVIIC 20 μM	RINGER
8	GLY + ω-contox MVIIC (n = 5)	RINGER	ω-contox MVIIC 40 μM	GLY 5 mM + ω-contox MVIIC 40 μM	RINGER
9	GLY + ω-contox GVIA (n = 5)	RINGER	ω-contox GVIA 20 μM	GLY 5 mM + ω-contox GVIA 20 μM	RINGER
10	GLY + ω-contox GVIA (n = 5)	RINGER	ω-contox GVIA 40 μM	GLY 5 mM + ω-contox GVIA 40 μM	RINGER

2.4. HPLC-ED analysis

The dopamine, DOPAC, and HVA levels were quantified by high-performance liquid chromatography with electrochemical detection (HPLC-EC) according to previous studies from our laboratory (Alfonso et al., 2019; Costas-Ferreira et al., 2023; Faro et al., 2018). Briefly, a

Jasco PU-1580 pump and a Reodyne 7125 injector were used, and a mobile phase (70 mM KH_2PO_4, 1 mM octanesulfonic acid, 1 mM EDTA, and 14% methanol; pH 3.4) was eluted through a 20 cm Spherisorb ODS-1 reverse phase column with 5 μm particle size. The dopamine, DOPAC and HVA detection was achieved by using an ESA Coulochem III 5100 A electrochemical detector with an oxidation potential of + 400 mV. All data were analyzed by the chromatographic software Cromanec XP 1.0.4 (Micronec, Spain).

2.5. Expression of results and statistics

Data were corrected using the percentage of in vitro recovery for every microdialysis probe, which was similar for the different type of probes used and for the substances analyzed: 13.7% for dopamine, 19.7% for DOPAC, and 21% for HVA. All values for the effects of GLY and VSCC antagonists on extracellular levels of dopamine, DOPAC, and HVA were expressed as the mean ± S.E.M. of 5–9 animals in each group. The average of basal levels of the three substances (defined as 100%) was determined from the two dialyzed samples prior to the addition of any drug or modified perfusion medium. Results were calculated as percentages of this mean basal release.

Statistical analysis of the results was performed by means of ANOVA and Scheffe *post-hoc* test, considering the following significant differences: * $P < 0.05$, * * $P < 0.01$, and * ** $P < 0.001$ with respect to the basal levels; $^{a}P < 0.05$, $^{b}P < 0.01$, and $^{c}P < 0.001$, with respect to the 5 mM GLY group.

2.6. Molecular docking

The ligands FLU (CID: 941361), ω-conotox GVIA (CID: 22834549), NIC (CID: 4474) and GLY (CID: 3496), obtained from the PubChem database (PBD, https://pubchem.ncbi.nlm.nih.gov), were optimized in the HyperChem software using the semi-empirical method of the type Recife model 1 (RM1) (Gutowska et al., 2005). For the calculation of molecular docking, the GOLD 2020.1 program (Genetic Optimization for Ligand Docking) was used, in order to predict the best interactions between the ligand and targets of interest (Ortega-Carrasco et al., 2014). The crystallographic structures were obtained from the Protein Data Bank (PDB) (Dong et al., 2021; He et al., 2022).

To evaluate the predictive capacity of the molecular docking method, a redocking was carried out with the purpose of establishing whether the program is able to determine the spatial orientation of the ligand, with its origin coordinates, in addition to the RMSD value (Root Mean Square Derivation) and validation radius. After validation, molecular docking was performed to evaluate the interactions and better poses of the ligand in the targets of interest.

3. Results

3.1. Effects of GLY on basal dopamine, DOPAC, and HVA release

Basal levels of dopamine and its metabolites in dialyzed samples were stable in control animals (non-treated rats). The mean of

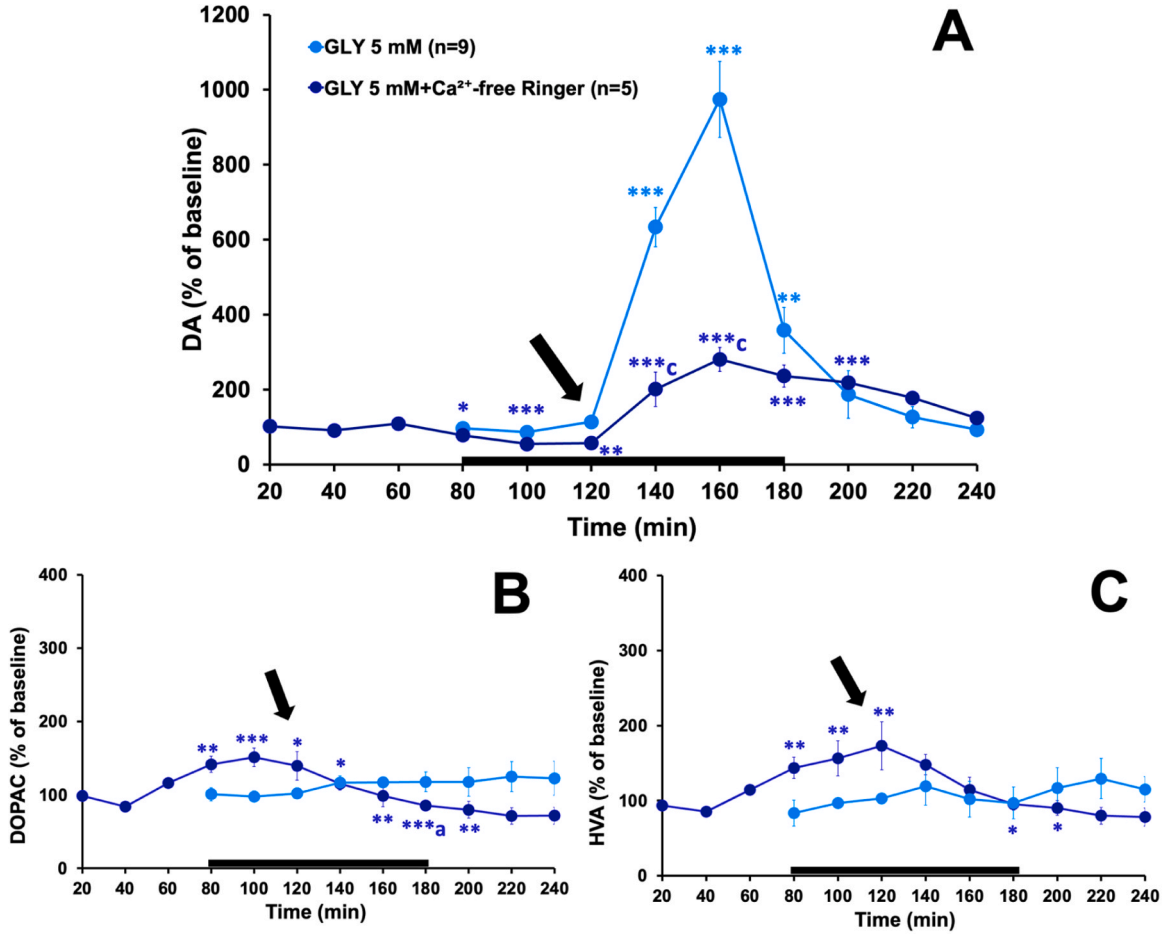

Fig. 1. Effects of 5 mM glyphosate (GLY) perfusion in a Ca^{2+}-free Ringer's solution on the dopamine (A), DOPAC (B), and HVA (C) levels in the rat striatum. Administration of Ca^{2+}- free Ringer solution is shown by the black bar and GLY infusion started at the time indicated by the arrow over 60 min. The results are shown as percentage of basal levels (100%). Basal levels were considered as the mean of dopamine, DOPAC, or HVA concentrations in the two samples before treatment perfusion. Significant differences: * $P < 0.05$, * * $P < 0.01$, and * ** $P < 0.001$, with respect to the basal level, and $^{c}P < 0.001$, with respect to 5 mM GLY control group.

dopamine, DOPAC, and HVA concentrations in the two samples collected before pesticide administration was considered as the basal level: 0.03 ± 0.008; DOPAC: 0.7 ± 015; HVA: 0.46 ± 0.09 ng/μL, respectively.

Intrastriatal infusion of GLY (5 mM, 60 min) through the microdialysis probe increased dopamine levels to 974.5 ± 152% ($p < 0.001$, t-test), compared to basal levels. This maximum increase was observed 40 min after the start of the pesticide infusion, and the basal values were recovered in the last 20 min of the experiment. In contrast, the administration of 5 mM GLY did not induce significant changes in the levels of dopamine metabolites. The data for the effects of GLY on striatal dopamine, DOPAC and HVA levels are plotted in Figs. 1–5 in order to compare them with the data obtained under other experimental conditions (treatments with antagonists together with GLY).

3.2. Role of external Ca^{2+} in the GLY-induced dopamine, DOPAC, and HVA release

To investigate if GLY-induced dopamine release was Ca^{2+}-dependent, a Ca^{2+}-free Ringer solution was infused through the dialysis probe. Fig. 1 shows the effect of Ca^{2+}-free Ringer solution infusion on extracellular levels of dopamine, DOPAC, and HVA. After removing Ca^{2+} from the perfusion medium, dopamine levels decreased significantly during three consecutive dialysates, leveling-off at 54.6 ± 11.2% ($p < 0.001$, t-test) of basal levels. These values were considered as basal for the measurement of GLY effects on dopamine release in Ca^{2+}-free medium. When GLY was perfused in Ca^{2+}-free Ringer solution, the striatal dopamine levels increased to 280.4 ± 32% ($p < 0.001$, t-test) with respect to the basal levels. One-way ANOVA analysis performed to compare the maximum effects of treatments confirmed that the removal of Ca^{2+} from the perfusion medium decreases the effect of the GLY: ($F(1,13) = 23.091$, $p < 0.001$.

Fig. 1B and 1 C show that removal of Ca^{2+} from the perfusion medium significantly increased DOPAC and HVA levels reaching a maximum value of 151.3 ± 12.5% ($p < 0.001$, t-test) and 173.1 ± 31.9% ($p < 0.01$, t-test) at 40 and 60 min, relative to baseline, respectively. When 5 mM GLY was administered in a Ca^{2+}-free medium, DOPAC and HVA levels decreased significantly to 85.4 ± 6.7% ($p < 0.001$, t-test) and 95.4 ± 8% ($p < 0.05$, t-test), with respect to basal levels, respectively. In the case of DOPAC, its levels were significantly lower than those observed after the administration of 5 mM GLY alone. One-way ANOVA analysis confirmed this difference: $F(1,12) = 8.673$, $p = 0.013$.

3.3. Role of T-type VSCC in the GLY-induced dopamine, DOPAC, and HVA release

To evaluate the role of T-type VSCC in the GLY-induced dopamine, DOPAC, and HVA release, we infused FLU, a blocker of these VSCC type, before and then together with 5 mM GLY through the microdialysis probe (Fig. 2). Intrastriatal administration of 10 or 100 μM FLU (for 60 min) had no significant effect on dopamine levels. As shown in

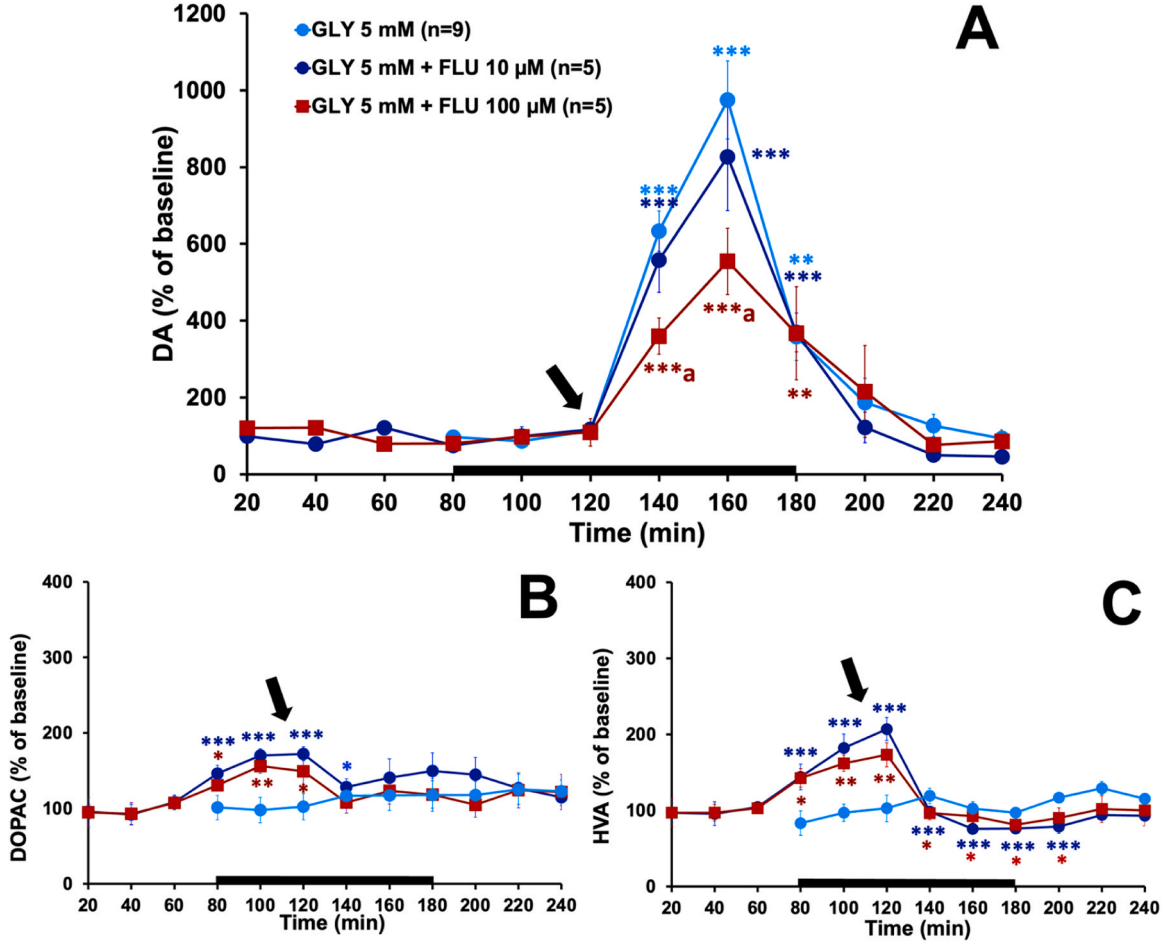

Fig. 2. Effects of 5 mM glyphosate (GLY) perfusion in flunarizine (FLU) pretreated animals on the dopamine (A), DOPAC (B), and HVA (C) extracellular levels in rat striatum. The FLU administration is shown by the black bar and GLY infusion started at the time indicated by the arrow over 60 min. The results are shown as percentage of basal levels (100%). Basal levels were considered as the mean of dopamine, DOPAC, or HVA concentrations in the two samples before drug administration. Significant differences: * $P < 0.05$, * * $P < 0.01$, and * ** $P < 0.001$, respect to basal levels; [a]$P < 0.05$, respect to 5 mM GLY group.

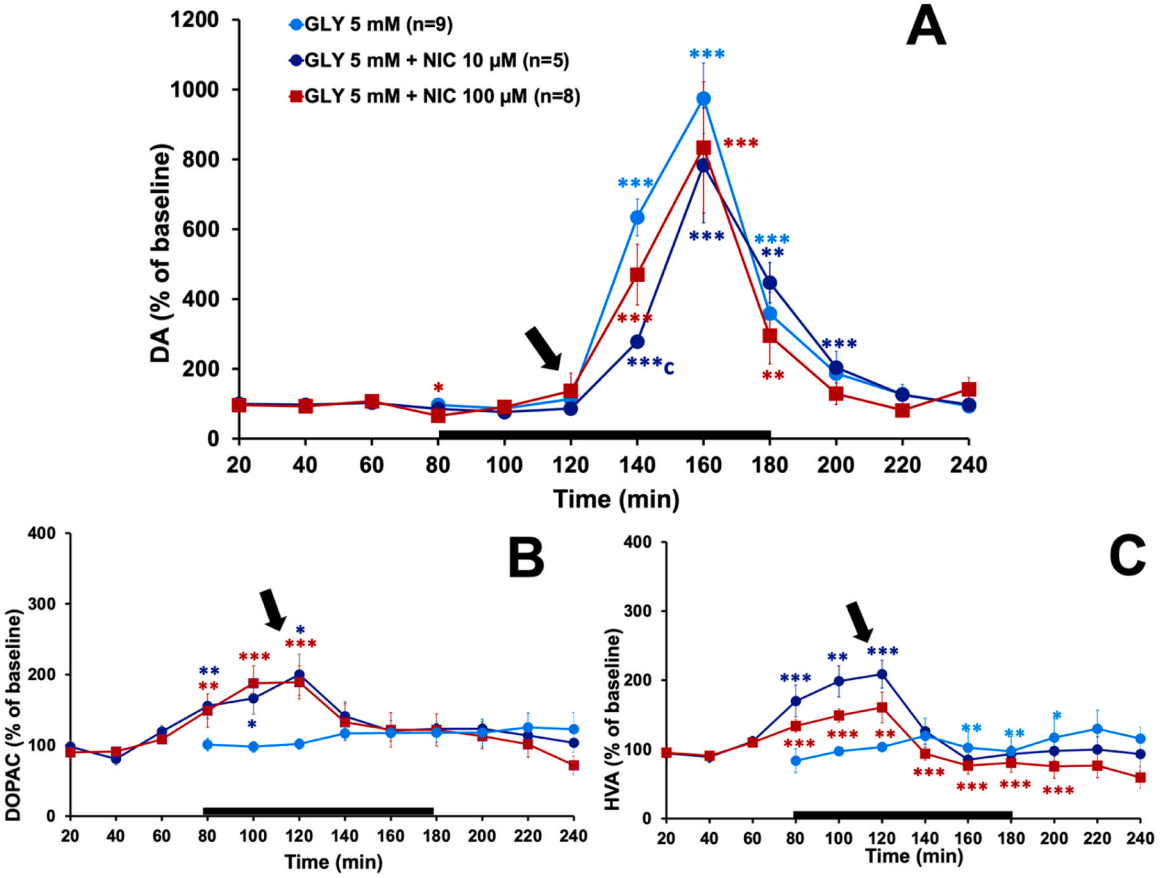

Fig. 3. Effects of 5 mM glyphosate (GLY) perfusion in nicardipine (NIC) pretreated animals on the dopamine (A), DOPAC (B), and HVA (C) extracellular levels in rat striatum. The NIC administration is shown by the black bar and GLY infusion started at the time indicated by the arrow over 60 min. The results are shown as percentage of basal levels (100%). Basal levels were considered as the mean of dopamine, DOPAC, or HVA concentrations in the two samples before drug administration. Significant differences: * $P < 0.05$, * * $P < 0.01$, and * ** $P < 0.001$, respect to basal levels; $^{c}P < 0.001$, respect to 5 mM GLY group.

Fig. 2A, when 5 mM GLY was administered to animals pretreated with 10 μM FLU, the dopamine levels increased to 827.1 ± 140.7% ($p < 0.001$, t-test), relative to baseline. On the other hand, the co-infusion of 100 μM FLU together with 5 mM GLY increased dopamine levels up to 554.8 ± 86.4% ($p < 0.001$, t-test), an increase significantly smaller than that obtained with GLY alone (974.5 ± 152%; $p < 0.05$) (Fig. 2A). One-way ANOVA analysis showed significant differences between the treatment groups [$F(2,18) = 3.813$; $p = 0.044$]. *Post-hoc* comparisons confirmed that administration of GLY to animals pretreated with 100 μM FLU induced increases in the dopamine levels that were significantly smaller than those observed with GLY alone: GLY vs 10 μM FLU+GLY: $p = 0.636$; GLY vs 100 μM FLU+GLY: $p = 0.044$).

Fig. 2B and 2 C show the effects of FLU and/or GLY on DOPAC and HVA levels. The administration of 10 and 100 μM FLU increased DOPAC levels up to 170.3 ± 14.7% ($p < 0.001$, t-test) and 156.3 ± 20.7% ($p < 0.01$, t-test) compared to baseline, respectively. Likewise, both concentrations of the antagonist (10 and 100 μM) also increased the extracellular levels of HVA to 182.3 ± 6.3% ($p < 0.001$, t-test) and 162.1 ± 19.3% ($p < 0.01$, t-test) compared to their baseline, respectively. Administration of 5 mM GLY to animals pretreated with 10 μM FLU produced a small but significant decrease in DOPAC levels up to 128 ± 11.1% ($p < 0.05$, t-test), compared to basal levels, while HVA levels decreased up to 75.8 ± 6.5% ($p < 0.001$, t-test) and 92.5 ± 8.1% ($p < 0.05$, t-test), for concentrations of 10 and 100 μM of FLU, respectively. In all cases, the effects observed were not significantly different from those observed with the administration of GLY alone. One-way ANOVA analysis confirmed that administration of GLY to animals pretreated with 10 or 100 μM FLU produced effects that were not statistically different from GLY group [DOPAC: $F(2,17) = 0.496$, $p = 0.618$; HVA: $F(2,20) = 1.010$, $p = 0.384$].

3.4. Role of L-type VSCC in the GLY-induced dopamine, DOPAC, and HVA release

To investigate the possible participation of L-type VSCCs in GLY-induced dopamine release, NIC, a blocker of these channels, was administered before and then together with 5 mM GLY through the microdialysis probe (Fig. 3). Intrastriatal administration of 10 μM NIC (for 60 min) had no significant effect on dopamine levels, while perfusion of 100 μM of this blocker significantly reduced extracellular dopamine levels to 65.5 ± 13.1% ($p < 0.05$, t-test), compared to basal values.

As shown in Fig. 3A, when 5 GLY was administered to animals pretreated with 10 or 100 μM NIC, the dopamine levels increased to 783 ± 165% ($p < 0.001$, t-test) and 834 ± 188% ($p < 0.001$, t-test), relative to basal levels, respectively. One-way ANOVA analysis also did not show significant differences between the treatment groups ($F(2,20) = 0.619$, $p = 0.550$). *Post hoc* comparisons confirmed that GLY-induced increases under L-type VSCC blocking conditions were not significantly different from those observed with GLY alone (GLY vs 10 μM NIC+GLY: $p = 0.607$; GLY vs 100 μM NIC+GLY: $p = 0.718$). As we observed with FLU, in this group of experiments, a significant difference was also observed between the effect of the co-infusion of NIC+GLY and GLY 20 min after the start of the pesticide infusion, but this difference has not been maintained in the following samples (Fig. 3A).

Administration of 10 μM NIC (for 60 min) induced significant

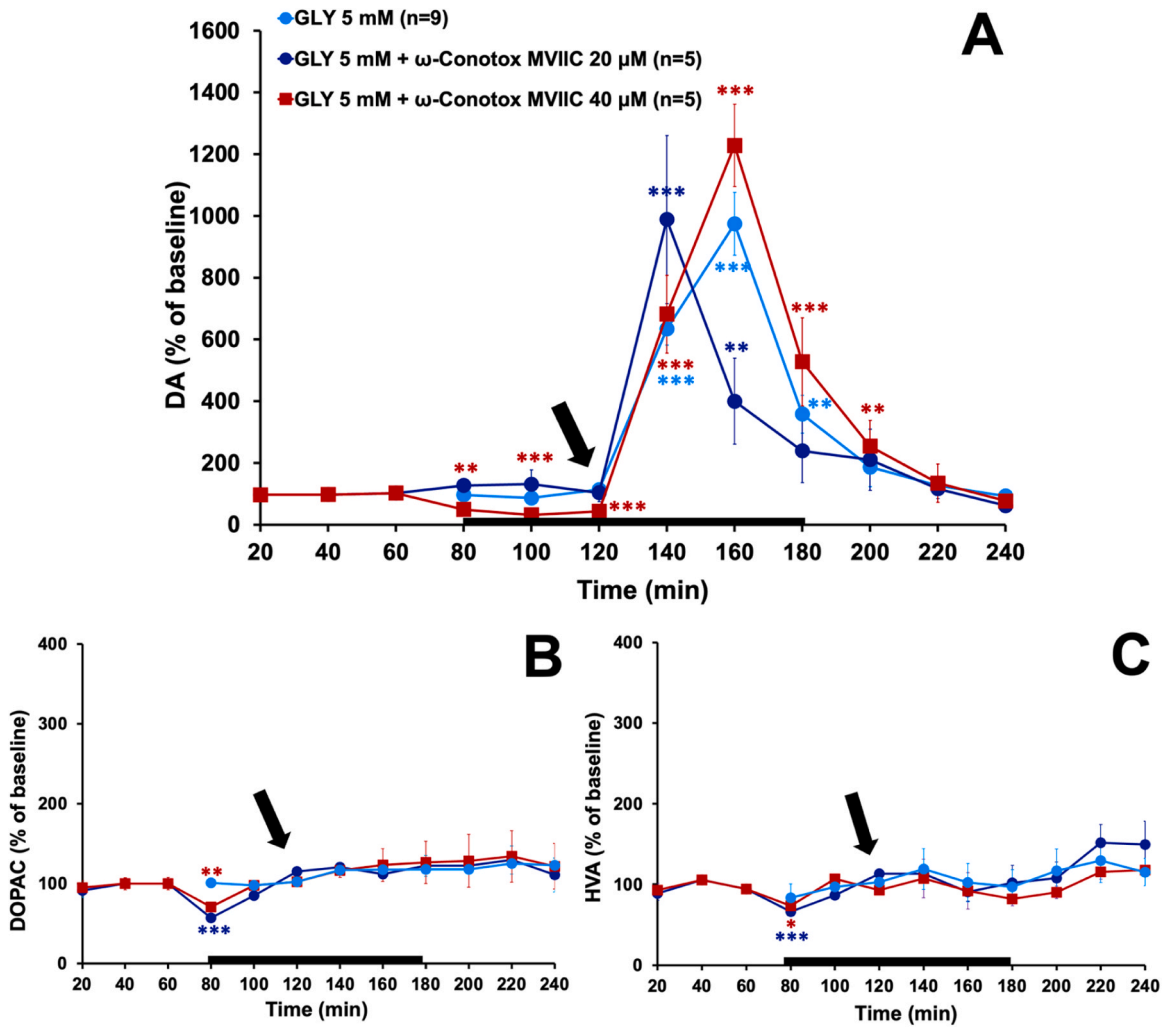

Fig. 4. Effects of 5 mM glyphosate (GLY) perfusion in ω-conotoxin MVIIC (ω-conotox MVIIC) pretreated animals on the dopamine (A), DOPAC (B), and HVA (C) extracellular levels in rat striatum. The ω-conotox GVIA administration is shown by the black bar and GLY infusion started at the time indicated by the arrow over 60 min. The results are shown as percentage of basal levels (100%). Basal levels were considered as the mean of dopamine, DOPAC, or HVA concentrations in the two samples before drug administration. Significant differences: * $P < 0.05$, * * $P < 0.01$, and * ** $P < 0.001$, respect to basal levels; $^{c}P < 0.001$, respect to 5 mM GLY group.

increases in DOPAC and HVA levels to 166.4 ± 22.2% ($p < 0.05$, t-test) and 198.4 ± 22.6% ($p < 0.01$, t-test), relative to baseline values, respectively. Similarly, the highest concentration of the antagonist (100 μM) also increased the extracellular levels of both DOPAC and HVA to 187.9 ± 24.8% ($p < 0.001$, t-test) and 148.6 ± 9.7% ($p < 0.001$, t-test), compared to the basal levels, respectively. On the other hand, although the administration of GLY to rats pretreated with 10 or 100 μM NIC did not produce significant changes in DOPAC levels, it decreased significantly HVA levels by up to 84.9 ± 10.4% ($p < 0.01$, t-test) and 76.2 ± 11.9% ($p < 0.001$, t-test), respectively (Figs. 3B and 3C). For both DOPAC and HVA, the one-way ANOVA analysis confirmed that administration of GLY to animals pretreated with 10 or 100 μM NIC produced effects that were not statistically different from GLY alone: DOPAC: $F(2,20) = 0.211$, $p = 0.811$; HVA: $F(2,22) = 1.283$, $p = 0.299$.

3.5. Role of P/Q-type VSCC in the GLY-induced dopamine, DOPAC, and HVA release

In the following set of experiments, GLY was administered to animals pretreated with ω-conotox MVIIC, a non-selective antagonist of P/Q-type VSCCs. Fig. 4A shows that administration of 20 μM ω-conotox MVIIC did not significantly change the dopamine levels, whereas infusion of 40 μM of the toxin significantly reduced dopamine levels to 31.5 ± 7.3% ($p < 0.001$, t-test), compared to basal levels. Infusion of 5 mM GLY in animals pretreated with 20 or 40 μM ω-conotox MVIIC increased dopamine levels to 988.4 ± 272% ($p < 0.001$, t-test) and 1128 ± 133% ($p < 0.001$, t-test), compared to the baseline, respectively. These increases were not statistically different from those seen with infusion of GLY alone. One-way ANOVA analysis also did not show significant differences between the treatment groups [$F(2,17) = 1.192$, $p = 0.331$]. *Post hoc* comparisons confirmed that GLY-induced increases under P/Q-type VSCC blocking conditions were not significantly different from those observed with GLY alone (GLY vs 20 μM ω-conotox MVIIC +GLY: $p = 0.963$; GLY vs 40 μM ω-conotox MVIIC +GLY: $p = 0.427$).

Fig. 4B and 4 C show that administration of 20 or 40 μM ω-conotox MVIIC (60 min) significantly reduced DOPAC [56.99 ± 2.1% ($p < 0.001$, t-test) and 70.6 ± 5.9% ($p < 0.01$, t-test)] and HVA [66.3 ± 2.7% ($p < 0.001$, t-test) and 73.6 ± 9.6% ($p < 0.05$, t-test)] levels, relative to basal levels, respectively. The perfusion of the GLY to the animals pretreated with both concentrations of ω-conotox MVIIC did not significantly modify the effect of the pesticide on the extracellular levels of DOPAC or HVA. One-way ANOVA analysis confirmed that administration of GLY to animals pretreated with 20 or 40 μM ω-conotox MVIIC

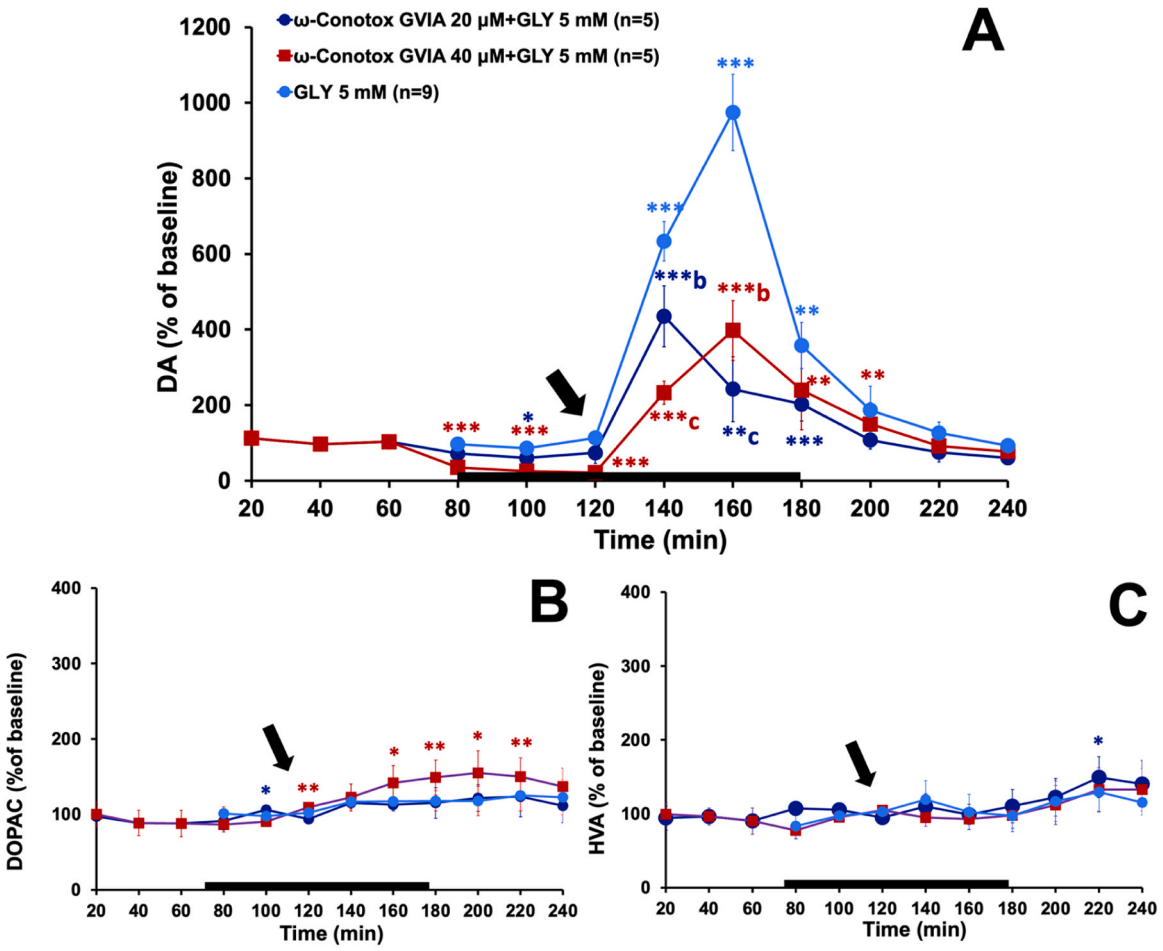

Fig. 5. Effects of 5 mM glyphosate (GLY) perfusion in ω-conotoxin GVIA (ω-conotox GVIA) pretreated animals on the dopamine (A), DOPAC (B), and HVA (C) extracellular levels in rat striatum. The ω-conotox GVIA administration is shown by the black bar and GLY infusion started at the time indicated by the arrow over 60 min. The results are shown as percentage of basal levels (100%). Basal levels were considered as the mean of dopamine, DOPAC, or HVA concentrations in the two samples before drug administration. Significant differences: * $P < 0.05$, * * $P < 0.01$, and * ** $P < 0.001$, respect to basal levels; $^{b}P < 0.01$ and $^{c}P < 0.001$, respect to 5 mM GLY group.

produced effects that were not statistically different from GLY alone: DOPAC: F(2,15) = 0.305, p = 0.934; HVA: F(2,18) = 0.216, p = 0.808.

3.6. Role of N-type VSCC in the GLY-induced dopamine, DOPAC, and HVA release

In the last set of experiments, the role of N-type VSCCs in GLY-evoked in vivo dopamine release was investigated. For this, the effect of GLY was studied in the presence of ω-conotox GVIA, a specific blocker of neuronal N-type VSCC. Our results show that the administration of 20 or 40 μM ω-conotox GVIA significantly reduced extracellular dopamine levels to 60.4 ± 24.2% ($p < 0.05$, t-test) and 21.6 ± 3.2% ($p < 0.001$, t-test), compared to baseline values, respectively. On the other hand, administration of 5 mM GLY to rats pretreated with 20 or 40 μM ω-conotox GVIA increased dopamine release to 435.5 ± 80.5% ($p < 0.001$, t-test) and 397.5 ± 78.7% ($p < 0.001$, t-test), relative to baseline values, respectively. Thus, the pretreatment with 20 or 40 μM ω-conotox GVIA significantly reduced the effect of GLY by 55.3% and 59.2%, respectively (Fig. 5A). One-way ANOVA analysis also showed significant differences between the treatment groups [F(2,20) = 13.698; p < 0.001]. *Post-hoc* comparisons confirmed that administration of GLY to animals pretreated with 20 or 40 μM ω-conotox GVIA induced increases in the dopamine levels that were significantly smaller than those observed with GLY alone: GLY vs 20 μM ω-conotox GVIA+GLY: p = 0.001; GLY vs 40 μM ω-conotox GVIA +GLY: p = 0.002.

Fig. 5B and 5 C show the effects of GLY in animals pretreated with 20 or 40 μM ω-conotox GVIA on DOPAC and HVA levels. The administration of both concentrations of the toxin had no significant effect on the levels of dopamine metabolites. The perfusion of GLY to the animals pretreated with 20 μM ω-conotox GVIA did not modify the DOPAC or HVA levels, while the concentration of 40 μM of the toxin increased the DOPAC levels up to 155 ± 29.3% ($p < 0.01$, t-test), with respect to the basal values, without altering the HVA levels. In all cases, the effects observed were not significantly different from those observed with the administration of GLY alone. One-way ANOVA analysis showed that administration of GLY to animals pretreated with ω-conotox GVIA produced effects that were not statistically different from GLY alone: DOPAC: F(2,15) = 2.927, p = 0.890; HVA: F(2,21) = 0.108, p = 0.898.

3.7. Molecular docking

Three crystallographic structures complexed with ligands were obtained in the PDB for further elucidation of the docking step. The first was the human low-voltage activated T-type VSCC ($Cav_{3.3}$) (PDB ID: 7WLL) with a resolution of 3.60 Å and complexed to pimozide (PMZ). The second refers to the human N-type VSCC ($Cav_{2.2}$) (PDB ID: 7VFV), with a resolution of 3.00 Å, and complexed to the ligand PD173212. And finally, the human L-type VSCC ($Cav_{1.3}$) (PDB ID: 7UHF), with a resolution of 3.10 Å and complexed with cinnarizine.

It is important to emphasize that molecular docking is a

computational approach aimed at enabling the assessment of the interaction between a low molecular weight molecule and a protein, for subsequent characterization of the potential behavior of the ligand in the active site, as well as predicting the biochemical processes that can arise from this interaction. In simplified terms, the analysis of docking is divided into two moments. The first refers to the evaluation of ligand poses, which basically involves elucidating the conformation, position, and orientation of the molecule within the active site (Meng et al., 2012). The GOLD program allows scoring different ligand conformations and determining which one fits best into the site (Verdonk et al., 2003). The other aspect is related to the assessment of the ligand's potential affinity for the target, through the score value, where the higher the value, the greater the indication of ligand-target affinity (Meng et al., 2012).

In the validation step, the $Cav_{3.3}$ low-voltage activated T-type VSCC (PDB ID: 7WLL), the RMSD value obtained was 0.630 Å. RMSD allows identifying and exploring the conformational space of a target and how the ligand behaves in that region (Guilbert and James, 2008). RMSD values below 2 Å are considered the most accepted, since it indicates that a correct fit of the ligand has occurred in a favorable spatial orientation in the protein (Hevener et al., 2009). The origin coordinates obtained for this target were: x = 134.94; y = 130.46; z = 139.27, in a radius of 10 Å.

In order to analyze the interaction between FLU, the antagonist used for the experimental assay with $Cav_{3.3}$, molecular docking was performed (Fig. 6). The score obtained was 73.40, with five types of interactions, hydrogen, halogen, and hydrophobic interactions (Table 2).

When molecular docking with GLY was performed (score: 37.72), a total of seven hydrogen interactions were observed, three with Lys1379, three with Asn850 and one Ser1419, which are stronger interactions due to the high polarity involved in the bond between a hydrogen and an electronegative atom, in addition to requiring a closer approximation for the interaction to occur (Yin et al., 2021). This demonstrates that depending on the type of interaction, the distances between the atoms of the ligand and the protein will vary, in which stronger interactions require a closer approximation, that is, the smaller the distance, the greater the indication of the force involved (Patrick, 2013).

As for the $Cav_{2.2}$ target (PDB ID: 7VFV), the RMSD result presented was in the amount of 2.617 Å. It is worth mentioning that even if this is above 2 Å, the value can be considered as within the limits of acceptability, since the structural characteristics of the binder can influence the alignment and this factor must be considered (Carugo and Pongor, 2008). The origin coordinates obtained for this target were: x = 161.59; y = 167.55; z = 153.25, with a radius of 10 Å.

To elucidate the action profile of GLY in the $Cav_{2.2}$ channel, a comparison was made between its docking with the antagonist ω-conotox GVIA, the blocker used experimentally. In all, nine interactions occurred, of which two were of the hydrogen type, with the amino acids Met1290 and Lys1280, and the remaining ones were all of the hydrophobic type with the residues Trp1219, Phe1272, Leu1222, Ile1225, Leu1256, Met1290, Leu1218 (Fig. 7).

Regarding docking with GLY, it was noticed that the degree of affinity was lower (score: 30.97) and the number of interactions as well, with a total of two hydrogen interactions, of the conventional type, with the amino acids Ser1696 and Ala1652.

The validation of the $Cav_{1.3}$ target (PDB ID: 7UHF) resulted in an RMSD value of 0.625 Å. In docking with NIC, a structure used experimentally as an L-type VSCC blocker, the occurrence of three hydrogen

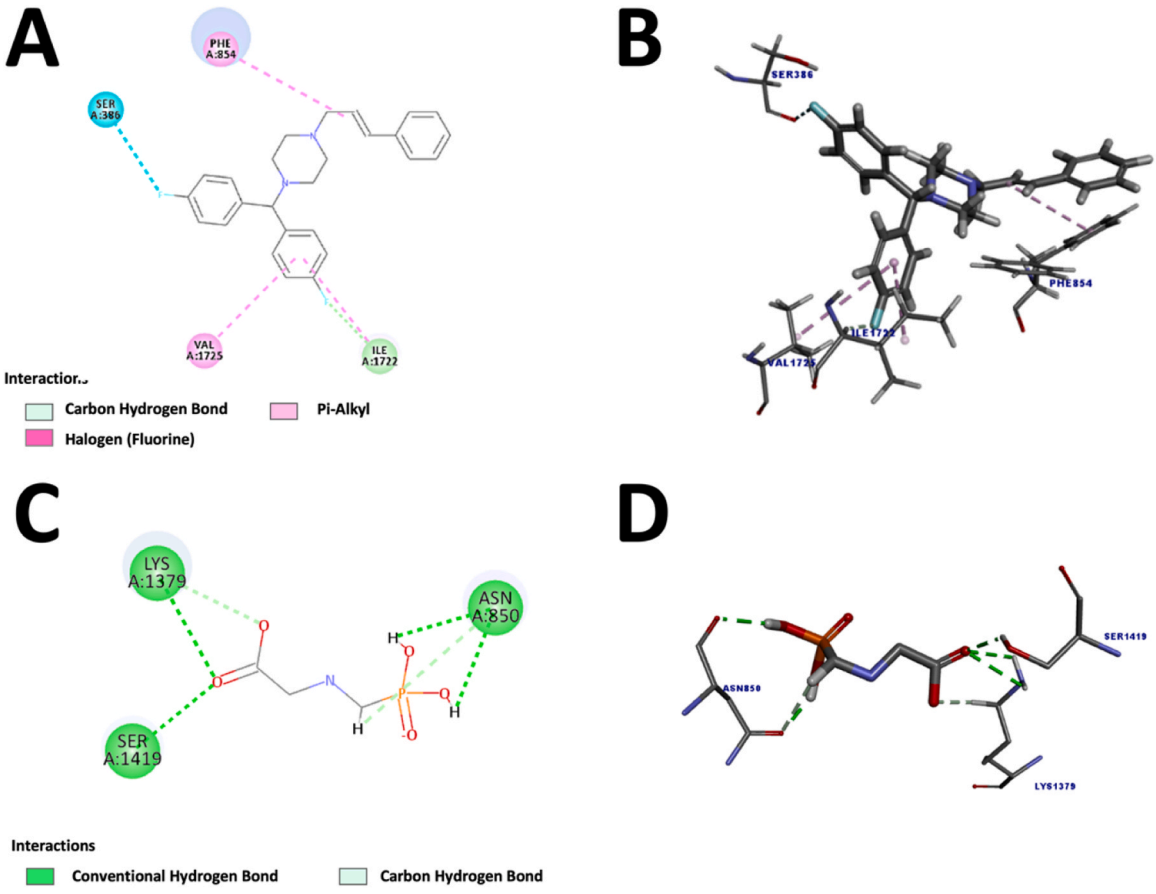

Fig. 6. Molecular docking of flunarizine (FLU) and glyphosate with $Cav_{3.3}$. (A) Molecular docking between FLU and the target, in 2D; (B) Molecular docking between FLU and the target, in 3D; (C) Molecular docking between glyphosate (GLY) and the target, in 2D; and (D) Molecular docking between GLY and the target, in 3D. Carbon-type intermolecular interactions are represented by light green color; conventional type in dark green; pi-alkyl type in light pink; and the halogen in blue.

Table 2
Interactions, types of interactions and docking score between different ligands in $Cav_{3.3}$, $Cav_{2.2}$, and $Cav_{1.3}$ channels. GLY, glyphosate; FLU, flunarizine; ω-conotox GVIA, ω-conotoxin GVIA; NIC, nicardipine.

Target	Ligand	Amino acids	Ligand atom	Interaction	Type	Distance	Score
7WLL	GLY	LYS1379	O6	Hydrogen bond	Conventional Hydrogen Bond	2.68	37.72
(Cav3.3)		LYS1379	O6	Hydrogen bond	Conventional Hydrogen Bond	2.74	
		SER1419	O6	Hydrogen bond	Conventional Hydrogen Bond	2.10	
		ASN850	H16	Hydrogen bond	Conventional Hydrogen Bond	2.12	
		ASN850	H17	Hydrogen bond	Conventional Hydrogen Bond	1.93	
		LYS1379	O5	Hydrogen bond	Carbon Hydrogen Bond	2.49	
		ASN850	H12	Hydrogen bond	Carbon Hydrogen Bond	2.87	
	FLU	ILE1722	F30	Hydrogen bond	Carbon Hydrogen Bond	2.35	
		SER386	F23	Halogen	Halogen (Fluorine)	3.58	73.90
		PHE854	Ligand	Hydrophobic	Pi-Alkyl	5.37	
		ILE1722	Ligand	Hydrophobic	Pi-Alkyl	5.08	
		VAL1725	Ligand	Hydrophobic	Pi-Alkyl	5.07	
7VFV	GLY	SER1696	H17	Hydrogen bond	Conventional Hydrogen Bond	1.76	30.97
(Cav2.2)		ALA1652	H18	Hydrogen bond	Conventional Hydrogen Bond	1.91	
	ω-conotox GVIA	MET129	H316	Hydrogen bond	Conventional Hydrogen Bond	1.69	74.03
		LYS1280	O191	Hydrogen bond	Carbon Hydrogen Bond	2.84	
		TRP1219	Ligand	Hydrophobic	Pi-Pi T-shaped	5.14	
		PHE1272	Ligand	Hydrophobic	Pi-Pi T-shaped	5.80	
		LEU1222	C1	Hydrophobic	Alkyl	3.87	
		ILE1225	C1	Hydrophobic	Alkyl	4.25	
		LEU1256	C1	Hydrophobic	Alkyl	5.14	
		MET1290	Ligand	Hydrophobic	Alkyl	3.91	
		LEU1218	Ligand	Hydrophobic	Pi-Alkyl	4.24	
7UHF	GLY	ASN740	O5	Hydrogen bond	Conventional Hydrogen Bond	2.03	34.96
(Cav1.3		THR703	H13	Hydrogen bond	Conventional Hydrogen Bond	1.99	
		GLU705	H16	Hydrogen bond	Conventional Hydrogen Bond	2.94	
		GLU1101	H16	Hydrogen bond	Conventional Hydrogen Bond	1.67	
		THR703	H17	Hydrogen bond	Conventional Hydrogen Bond	1.61	
		LEU702	H18	Hydrogen bond	Conventional Hydrogen Bond	2.97	
		GLU705	O2	Hydrogen bond	Carbon Hydrogen Bond	2.96	
	NIC	ASN740	O11	Hydrogen bond	Conventional Hydrogen Bond	1.86	55.02
		ASN740	N14	Hydrogen bond	Conventional Hydrogen Bond	2.13	
		PHE736	C16	Hydrogen bond	Carbon Hydrogen Bond	3.74	
		ILE737	Ligand	Hydrophobic	Pi-sigma	2.67	
		PHE1100	Ligand	Hydrophobic	Pi-Pi T-shaped	5.42	

and two hydrophobic interactions was observed, the first with residues Asn740 and Phe763, and the last between Ile737 and Phe1100. When docked with GLY, a greater number of interactions occurred, all of which were carbon-type hydrogen bonds (Fig. 8). Despite being interactions that require a closer approximation of the ligand, the affinity with $Cav_{1.3}$ (score 34.96) was not high, even presenting a similar score profile when compared to other dockings that were performed with GLY.

4. Discussion

4.1. Effects of GLY on in vivo dopamine release

In previous studies we have shown that intrastriatal administration of GLY increased the in vivo dopamine release from dorsal striatum in a concentration-dependent manner (Costas-Ferreira, 2023). According to this data, GLY-induced dopamine release is not dependent on membrane depolarization and appears to be partially dependent on the presence of dopamine in synaptic vesicles. In addition, the results also indicate that GLY acts on the dopamine transporter, modifying its activity to increase levels of the neurotransmitter in the extracellular medium. Here, we completed this information by demonstrating that the GLY-induced increases in dopamine levels are largely dependent on the presence of Ca^{2+} in the external medium, since the removal of these ions from the perfusion medium decreased the pesticide's effect on striatal dopamine release by 71% (Fig. 1). This result indicates that influx of Ca^{2+} through the different types of striatal channels and receptors could play an important role in the effect of GLY on dopaminergic neurotransmission. Thus, in the following experimental groups, we evaluated the role of VSCCs in the effect of GLY on in vivo release of dopamine and its metabolites. Our results show that blocking T-type channels with FLU (100 μM) or N-type channels with ω-conotox GVIA (10 and 100 μM) significantly decreased the effect of GLY on dopamine release in the dorsal striatum.

There is a great heterogeneity of VSCCs that participate directly or indirectly in the process of neurotransmission, but it is the N- and P/Q-type channels that appear to play a dominant role in the CNS, although other channels such as L- or T-type also regulate neurotransmitter release in some neurons (Pan et al., 2001; Rusakov, 2006; Tang et al., 2011; Tippens et al., 2008). In the striatum, dopamine transmission is also controlled by different types of VSCCs, including N-, P/Q-, T-, and L-type channels, which play distinct roles in modulating nigrostriatal dopaminergic neurotransmission. However, N-type channels are the main responsible for dopamine release, as their blockade almost completely eliminates neurotransmitter release (Brimblecombe et al., 2015; Phillips and Stamford, 2000).

Although traditionally the activity of type T VSCCs has been associated with the regulation of membrane excitability and neuronal oscillatory activity, growing evidence suggests that this type of channel can also mediate exocytosis (Pan et al., 2001; Tang et al., 2011; Weiss et al., 2012). In this sense, it has been shown that, in the striatum, T-type channels influence dopamine release, as their blockade modestly reduces neurotransmitter release, although it does not completely suppress it (Brimblecombe et al., 2015). In the present study, we observed that the blockade of T-type VSCCs with FLU significantly reduced the GLY-induced dopamine release, suggesting the involvement of this type of channel in the pesticide's effect. However, it should be noted that although FLU acts mainly as an antagonist of T-type VSCCs, at high concentrations its blocking capacity can extend to other VSCCs (L-, N-, and P/Q-type) and even to voltage-dependent sodium channels (Geer et al., 1993). Therefore, since in the present research only the highest concentration of FLU (100 μM) reduced the effect of GLY, we must consider the hypothesis that this effect is also due to non-specific

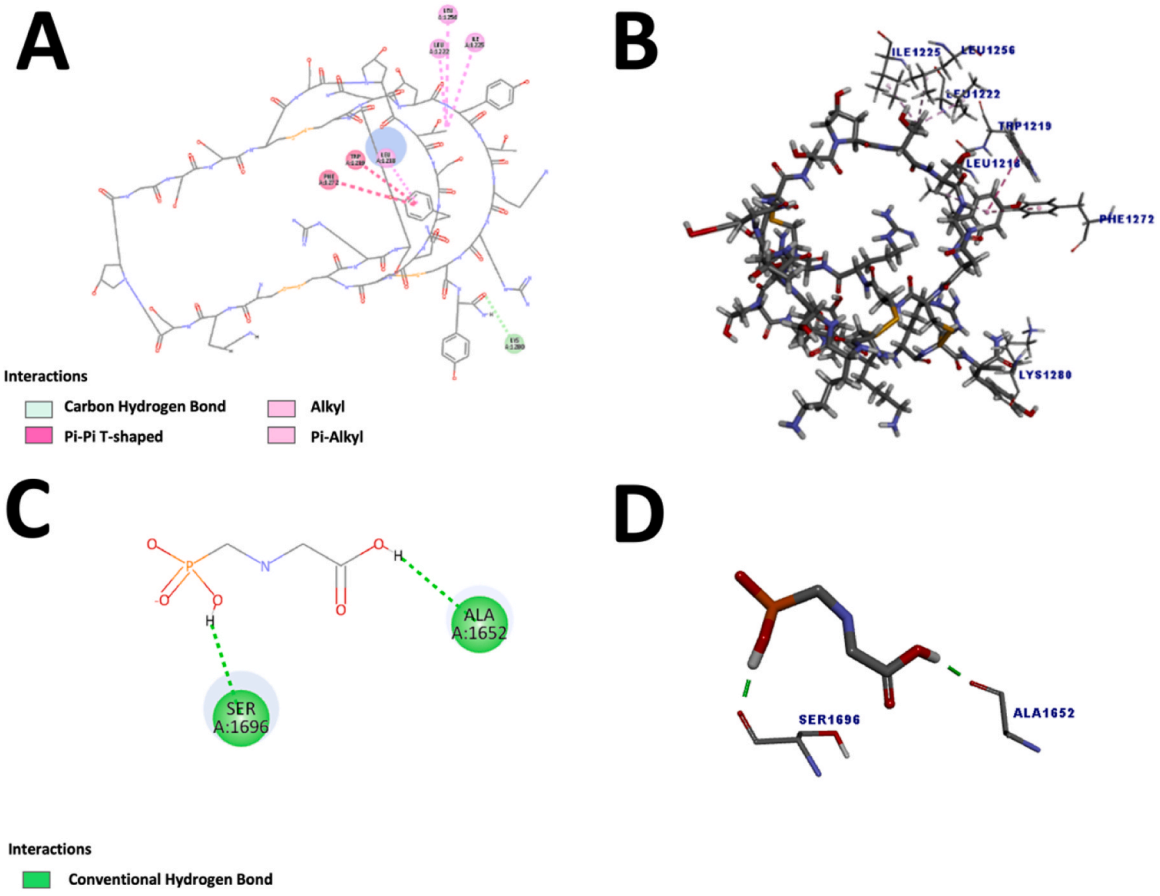

Fig. 7. Molecular docking of ω-conotoxin GVIA (ω-conotox GVIA) and glyphosate (GLY) with $Cav_{2.2}$. (A) Molecular docking between ω-conotox GVIA and the target in 2D; (B) Molecular docking between ω-conotox GVIA and the target, in 3D; (C) Molecular docking between GLY and the target, in 2D; and (D) Molecular docking between GLY and the target, in 3D. Carbon-type intermolecular interactions are represented by light green color; conventional type in dark green; the pi-pi T-shaped in dark pink; and the alkyl and pi alkyl type in light pink.

blockade of other channels and not exclusively to type T channels.

Another type of channel expressed by nigrostriatal dopaminergic neurons are L-type VSCCs (Dryanovski et al., 2013; Takada et al., 2001). While traditionally it was thought that this type of VSCC was not involved in neurotransmission (de Erausquin et al., 1992; Kimura et al., 1995), more recent studies suggest that the activity of L-type channels located in dopaminergic axons can actively contribute to induce dopamine release from striatum (Brimblecombe et al., 2015, 2020; Okita et al., 2000). However, in the present study, blocking L-type VSCCs with NIC (10 or 100 μM) did not modify the effect of GLY on dopamine release, which could indicate that these channels are not recruited by the pesticide to induce neurotransmitter release.

According to the available literature, the influx of Ca^{2+} through N- and P/Q-type channels is responsible for triggering all the machinery required for striatal dopamine release, so it is expected that their blockade will seriously affect dopaminergic neurotransmission. Regarding P/Q-type channels, our results show that the ω-conotox MVIIC did not alter the effect of GLY, questioning the mediating role of this type of VSCC in the pesticide's effect on dopamine release under our experimental conditions. Instead, we observed that the administration of 10 or 100 μM of ω-conotox GVIA reduced the effect of GLY by ~55% and ~60%, respectively (Fig. 5), indicating the important role of N-type VSCCs in the pesticide's effect on in vivo dopamine release. These results are consistent with previous studies in which N-type VSCCs had the greatest effect on dopamine release from striatal terminals (Brimblecombe et al., 2015; Phillips and Stamford, 2000).

Taken together, our results suggest that in vivo dopamine release induced by GLY could occur through an exocytotic process that is dependent on Ca^{2+} entry through some of the VSCCs located at the dopaminergic terminals. Overall, this release appears to depend primarily on N-type VSCCs, although other VSCCs such as T-type may also play an active role in the pesticide's effect. However, it is important to note that the contribution of each VSCC type to dopamine release is not fixed but varies dynamically depending on various factors such as neuronal activity or the probability of dopamine release (Brimblecombe et al., 2015). Thus, under physiological conditions, striatal dopamine release appears to depend mainly on N- and P/Q-type VSCCs, with the involvement of L- and T-type channels. However, we also hypothesize that the overstimulation of dopaminergic neurons induced by GLY may alter the usual dynamics of VSCC functioning, which could explain the results observed here.

Another important aspect is that, in the present study, the maximum reduction in the effect of GLY observed after the removal of Ca^{2+} from the perfusion medium or the administration of the antagonists was approximately 50–70%. This means that neither the administration of specific antagonists nor the reduction of Ca^{2+} from the extracellular medium were able to completely abolish the GLY-induced dopamine release. This could indicate the existence of mechanisms other than Ca^{2+}-dependent exocytotic release that could mediate GLY-induced dopamine release in the striatum.

The available literature describes that GLY can cause damage to the CNS through multiple mechanisms, including increases in levels of glutamate and acetylcholine, by inhibiting the reuptake and/or activity of enzymes involved in the degradation of these neurotransmitters (Ait-Bali et al., 2020, 2019; Cattani et al., 2017, 2014; Gallegos et al., 2020; Larsen et al., 2016). Increases in the extracellular levels of both

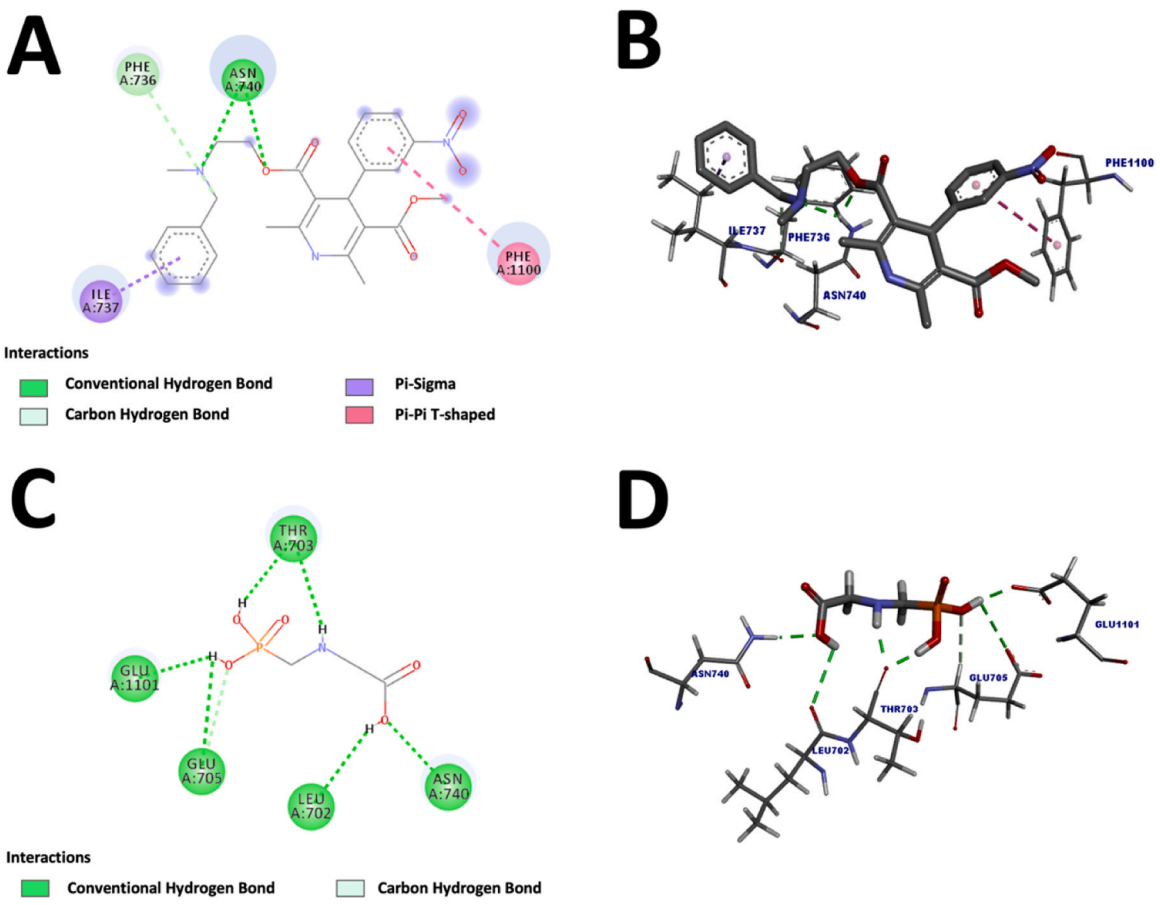

Fig. 8. Molecular docking of nicardipine (NIC) and glyphosate (GLY) with $Cav_{1.3}$. (A) Molecular docking between NIC and the target, in 2D; (B) Molecular docking between NIC and the target, in 3D; (C) Molecular docking between GLY and the target, in 2D; and (D) Molecular docking between GLY and the target, in 3D. Carbon-type intermolecular interactions are represented by light green color; conventional type in dark green; the pi-pi T-shaped in dark pink; and the pi-sigma type in purple.

neurotransmitters can activate both nicotinic acetylcholine receptors (nAChR) and NMDARs. In fact, it has been shown that GLY itself can bind to the cavities of NMDAR and produce their opening (Cattani et al., 2017).

Additionally, both nAChRs and NMDARs are differentially permeable Ca^{2+} ion channels, which play a critical role in regulating dopamine release in the striatum since both modulate the entry of this ion into dopaminergic terminals. In this regard, there is abundant evidence supporting the mediating role of some nAChRs and the NMDARs at dopaminergic terminals in the striatal dopamine release (Chéramy et al., 1996; Krebs et al., 1991; Martínez-Fong et al., 1992; Nolan et al., 2020; Turner, 2004). Thus, during exposure to GLY, the influx of Ca^{2+} to the dopaminergic terminal might not occur exclusively through the VSCCs, but also through some glutamatergic and cholinergic ionotropic receptors.

Impaired motor function is one of the most common behavioral consequences of GLY exposure. In the basal ganglia, dopaminergic pathways that project from the midbrain to the striatum are primarily responsible for movement control. Therefore, any imbalance in the functioning of these pathways, such as excessive GLY-induced dopamine release, could lead to loss of normal movement and impaired locomotion (Aoyama et al., 2000). Furthermore, as a highly reactive molecule, when its concentrations are high and exceed the mechanisms that cells must neutralize it, dopamine can be rapidly oxidized and produce reactive oxygen species that generate oxidative stress and consequent neuronal damage (Meiser et al., 2013; Monzani et al., 2019).

Oxidative stress in the nervous system after GLY exposure has been reported in numerous in vivo and in vitro animal and human studies (Cattani et al., 2017, 2014; Costas-Ferreira et al., 2023; Faria et al., 2021; Gallegos et al., 2020; Martínez et al., 2020; Sobjak et al., 2017). Ultimately, oxidative stress could lead to the degeneration of dopaminergic neurons, which could explain the development of persistent impairment of motor behavior and, in particular, the parkinsonism observed in some individuals long after exposure to GLY (Barbosa et al., 2001; Eriguchi et al., 2019; Zheng et al., 2018).

In summary, these results demonstrate that the release of dopamine induced by exposure to GLY is a process partially dependent on the extracellular Ca^{2+} ions. The interpretation of our results considering the available literature suggests that the pesticide can induce the influx of Ca^{2+} into the cell through different pathways, including VSCCs. Likewise, the need for further research in this area is also highlighted, with the aim of identifying the other pathways through which GLY induces dopamine release, such as the possible mediation of the glutamatergic and cholinergic systems.

4.2. *Molecular docking*

According to the study by He et al. (2022), three molecules with potential antagonistic activity under $Cav_{3.3}$ and with different pharmacological properties, were complexed to the target, to compare the intermolecular interactions. The first refers to mibeferadil, an antihypertensive drug derived from tretalin replaced by benzimidazole. Mibeferadil showed hydrogen interactions with the amino acid residues Leu818, Asn850, Lys1379 and Ser1419 from $Cav._{3.3}$ and hydrophobic interactions with other surrounding amino acids in the region, Phe854, Leu818, Leu1451, Phe1426, Leul721 and Ile1722. These interactions, in

turn, enabled a better fit of the molecule and allowed its stabilization in the site, thus causing a probable blocking effect on the channel. As for the second molecule highlighted in the study, otilonium bromide, which has antispasmodic properties, interacted through hydrogen bonds with the amino acids Lys1379 and Leu818. Structurally, otilonium bromide has N-octyloxy, benzoyl, benzocaine, and quaternary ammonium groups, which allow better access to the binding site and form hydrophobic interactions with nearby amino acids, causing channel blockage and subsequent inactivation. Finally, the molecule mentioned in the study, pimozide, which has potential antipsychotic activity, is formed by a benzimidazole group (like mibeferadil), a piperidinyl and two fluorophenyl groups. The benzimidazole group interacts with residues Leu818 and Asn850 through hydrogen bonds and with amino acids Phe815, Phe854 and Leu1415, hydrophobic bonds, enabling better coupling at the site. The other groups also interact through hydrophobic bonds, Val858, Leu1423, Phe1426, Ile1722 and Val1725.

As FLU has a high affinity with the site, it manages to fit into a favorable conformation, thus allowing a blocking action on the channel, which even, through the experimental assay, this action was proven. GLY, in turn, interacted, through hydrogen bonds, with most of the amino acid residues mentioned in the study by He et al. (2022) (Fig. 6), however, it is not possible to establish that GLY presents an antagonistic profile against the $Cav_{3.3}$ target, given its smaller size and because it does not have chemical groups in its structure that allow other interactions, mainly hydrophobic ones, if compared to other known channel antagonists.

In addition, even though it presented more interactions when compared to FLU, the GLY score was lower, indicating that it has less affinity with the channel, and therefore, less potential to block it, but that even under these conditions, it can exert some effect that influences the dopamine release, even if the channel is blocked with a specific antagonist, such as FLU.

In the study carried out by Dong et al. (2021), the ligand PD173212, a potent selective blocker of the $Cav_{2.2}$ channel, which has phenyl, tyrosamide and 4-tertbutylbenzyl groups in its structure, was complexed to the $Cav_{2.2}$ VSCC. Amino acids that can play an important role in determining antagonist activity are diverse, such as Phe345, Leu352, Ser1696, Phe1697, Phe1693, Tyr1298, Phe1411, Val1408, Val1412, Thr1363, Phe1359, Leu1700, Phe1703, many of which interact through bonds hydrophobic and Van der Wals.

In another study, molecular docking of cannabidiol with the $Cav_{2.2}$ protein was performed and the formation of hydrogen bonds with Leu1352 and Leu1356, alkyl interactions with residues Leu1352, Leu1356 and Met1293, five interactions of the π-alkyl type with Phe1693, Phe1359, Val1689, Leu1356 and Trp1353 and a π-sigma interaction with Tyr1685. Regarding the spatial orientation of the ligand, it was noticed that cannabidiol did not perform hydrophobic interactions, such as Trp768, Ser764-Ala783, Tyr1289 and Phe1411, which are considered critical to cause inhibition, when compared to other antagonists such as ziconotide and PD173212 itself. According to the author, because cannabidiol causes less pore occlusion and does not produce any stabilization in the channel, mainly due to hydrophobic bonds, it does not produce direct inhibition in $Cav_{2.2}$ (Harding et al., 2023).

Since ω-conotox GVIA is a high molecular weight molecule and spatially occupies a large space at the site, it manages to block the channel more easily, which can be confirmed by the score itself (74.03), which demonstrates high affinity with the target.

With the structural differences between GLY and other antagonists, mainly the one used experimentally (ω-conotox GVIA), a reduced number of interactions is to be expected. However, even so, GLY still has a certain degree of affinity with the site, which allows it to exert some effect on the channel, even after blocking (Fig. 7).

According to the study by Yao et al. (2022), when performing the docking between $Cav_{1.3}$ and the blocker of this channel, cinnarizine, it was observed that the ligand was spatially located in the pore domain, aligned just below of the selectivity filter region, blocking the ion conduction path. The site has a hydrophobic pocket composed of several amino acids, such as Phe699, Leu702, Leu743, Leu744, Phe747, Ile1136, Ile1137, Ala1140 and Met1144. The cinnarizine diphenylmethane group occupied this region, allowing its blockade. Hydrogen interaction was also observed between the piperazine group and the Asn740 residue and between the cinnamyl group, which was located in the region between the Met363 and Phe1100 residues, close to the selectivity filter region.

Even though the affinity potential of NIC with the target was 55.02, which indicates lower interaction affinity compared to FLU and ω-contox GVIA, NIC still exerts a blocking effect on the channel and for this reason the GLY can interact better with the target, influencing the dopamine release observed with brain microdialysis.

Overall, in view of our findings, we can indicate that GLY stimulates dopamine release through its interaction with certain types of VSCC. The possibility that the action of GLY could alter neurotransmission processes in mammals could highlight the need to evaluate the dangers of exposure to this substance and even reconsider established exposure limits. Furthermore, the identification of new molecular targets of glyphosate action in non-target organisms could be useful for the development of more appropriate therapeutic strategies.

5. Conclusion

In the present study we evaluated whether the in vivo release of dopamine induced by GLY in the dorsal striatum of rats depends on the activation of the different types of VSCC present in the dopaminergic terminal. To this end, selective blockers of type T, L, N and P/Q VSCCs were administered. Our findings suggest that GLY-induced dopamine release depends, at least in part, on the presence of Ca^{2+} in the external environment and its influx through T-type VSCCs and, especially, N-type VSCCs, since blocking each of these channels significantly reduced the pesticide-induced release of dopamine.

To explain these experimental results, the fact that the FLU and ω-contox GVIA antagonists have higher affinity for the targets (score of 73.90 and 74.03, respectively) compared to the GLY docking, can be inferred that these antagonists possibly prevent, with greater force, the interaction of the GLY with the VSCCs, which induces the decrease in dopamine release observed experimentally. On the other hand, when evaluating the L-type VSCC, it is noted that the antagonist (NIC) has lower affinity with the target (Score of 55.02), allowing the GLY to interact with the protein more easily, which could stimulate the release of the neurotransmitter, a result that would also corroborate the results obtained with brain microdialysis.

CRediT authorship contribution statement

C. Costas-Ferreira has carried out the microdialysis experiments, analyzed the data, wrote, and reviewed the manuscript; A.C.J. Silva and L.I.S. Hage-Melim were responsible for carrying out the molecular docking and the analysis of the results obtained; L. R. F. Faro responsible for funding acquisition; designed the study, analyzed all the data, wrote, and reviewed the manuscript.

Declaration of Competing Interest

The authors declare that they have no known competing financial interests or personal relationships that could have appeared to influence the work reported in this paper.

Data Availability

No data was used for the research described in the article.

Acknowledgements

The research was supported by grant from Xunta de Galicia (ED431B2019/33). Carmen Costas-Ferreira acknowledges University of Vigo for a scholarship.

References

Ait-Bali, Y., Kaikai, N., Ba-M'hamed, S., Bennis, M., 2019. Learning and memory impairments associated to acetylcholinesterase inhibition and oxidative stress following glyphosate based-herbicide exposure in mice. Toxicology 415, 18–25. https://doi.org/10.1016/j.tox.2019.01.010.

Ait-Bali, Y., Ba-M'hamed, S., Gambarotta, G., Sassoè-Pognetto, M., Giustetto, M., Bennis, M., 2020. Pre- and postnatal exposure to glyphosate-based herbicide causes behavioral and cognitive impairments in adult mice: evidence of cortical ad hippocampal dysfunction. Arch. Toxicol. 94, 1703–1723. https://doi.org/10.1007/s00204-020-02677-7.

Alfonso, M., Durán, R., Fajardo, D., Justo, L., Faro, L.R., 2019. Mechanisms of action of paraoxon, an organophosphorus pesticide, on in vivo dopamine release in conscious and freely moving rats. Neurochem Int 124, 130–140. https://doi.org/10.1016/j.neuint.2019.01.001.

Aoyama, S., Kase, H., Borrelli, E., 2000. Rescue of locomotor impairment in dopamine D2 receptor-deficient mice by an adenosine A2A receptor antagonist. J. Neurosci. 20, 5848–5852. https://doi.org/10.1523/JNEUROSCI.20-15-05848.2000.

Arias, B., Durán, R., Alfonso, M., 1998. In vivo release of dopamine and its metabolites from rat striatum in response to domoic acid. Neurochem Res 23, 1509–1514. https://doi.org/10.1023/A:1020919818652.

Barbosa, E.R., Leiros da Costa, M.D., Bacheschi, L.A., Scaff, M., Leite, C.C., 2001. Parkinsonism after glycine-derivate exposure. Mov. Disord. 16, 565–568. https://doi.org/10.1002/mds.1105.

Becker, J.B., Prendergast, B.J., Liang, J.W., 2016. Female rats are not more variable than male rats: a meta-analysis of neuroscience studies. Biol. Sex. Differ. 7, 1–7 https://doi.org/10.1186%2Fs13293-016-0087-5.

Bergquist, F., Jonason, J., Pileblad, E., Nissbrandt, H., 1998. Effects of local administration of L-, N-, and P/Q-type calcium channel blockers on spontaneous dopamine release in the striatum and the substantia nigra: a microdialysis study in rat. J. Neurochem 70, 1532–1540. https://doi.org/10.1046/j.1471-4159.1998.70041532.x.

Brimblecombe, K.R., Gracie, C.J., Platt, N.J., Cragg, S.J., 2015. Gating of dopamine transmission by calcium and axonal N-, Q-, T- and L-type voltage-gated calcium channels differs between striatal domains. J. Physiol. 593, 929–946. https://doi.org/10.1113/jphysiol.2014.285890.

Brimblecombe, K.R., Connor-Robson, N., Roberts, B.M., Gracie, C., Naude, R., te, W., Karthik, G., Wade-Martins, R., Cragg, S.J., 2020. L-type calcium channel contribution to striatal dopamine release is governed by calbindin-D28K, the dopamine transporter, D2-receptors, α2δ-subunits and sex differences. bioRxiv. https://doi.org/10.1101/2020.07.03.186411.

Burley, J.R., Dolphin, A.C., 2000. Overlapping selectivity of neurotoxin and dihydropyridine calcium channel blockers in cerebellar granule neurones. Neuropharmacology 39, 1740–1755. https://doi.org/10.1016/s0028-3908(99)00266-x.

Campos, F., Duran, R., Vidal, L., Faro, L.R.F., Alfonso, M., 2007. In vivo neurochemical characterization of anatoxin-a evoked dopamine release from striatum. J. Neural Transm. 114, 173–184. https://doi.org/10.1007/s00702-006-0542-2.

Carugo, O., Pongor, S., 2008. A normalized root-mean-spuare distance for comparing protein three-dimensional structures. Protein Sci. 10, 1470–1473. https://doi.org/10.1110/ps.690101.

Cattani, D., de Liz Oliveira Cavalli, V.L., Heinz Rieg, C.E., Domingues, J.T., Dal-Cim, T., Tasca, C.I., Mena Barreto Silva, F.R., Zamoner, A., 2014. Mechanisms underlying the neurotoxicity induced by glyphosate-based herbicide in immature rat hippocampus: involvement of glutamate excitotoxicity. Toxicology 320, 34–45. https://doi.org/10.1016/j.tox.2014.03.001.

Cattani, D., Cesconetto, P.A., Tavares, M.K., Parisotto, E.B., De Oliveira, P.A., Rieg, C.E. H., Leite, M.C., Prediger, R.D.S., Wendt, N.C., Razzera, G., Filho, D.W., Zamoner, A., 2017. Developmental exposure to glyphosate-based herbicide and depressive-like behavior in adult offspring: implication of glutamate excitotoxicity and oxidative stress. Toxicology 387, 67–80. https://doi.org/10.1016/j.tox.2017.06.001.

Chéramy, A., Godeheu, G., L'Hirondel, M., Glowinski, J., 1996. Cooperative contributions of cholinergic and NMDA receptors in the presynaptic control of dopamine release from synaptosomes of the rat striatum. J. Pharm. Exp. Ther. 276, 616–625.

Costas-Ferreira, C., Durán, R., Faro, L.R.F., 2023. Neurotoxic effects of exposure to glyphosate in rat striatum: effects and mechanisms of action on dopaminergic neurotransmission. Pest Biochem. Physiol. 193, 105433 https://doi.org/10.1016/j.pestbp.2023.105433.

Dong, Y., Gao, Y., Xu, S., Wang, Y., Yu, Z., Li, Y., Li, B., Yuan, T., Yang, B., Zhang, X.C., Jiang, D., Huang, Z., Zhao, Y., 2021. Closed-state inactivation and pore-blocker modulation mechanisms of human $CaV_{2.2}$. Cell Rep. 37, 109931 https://doi.org/10.1016/j.celrep.2021.109931.

Dryanovski, D.I., Guzman, J.N., Xie, Z., Galteri, D.J., Volpicelli-Daley, L.A., Lee, V.M.-Y., Miller, R.J., Schumacker, P.T., Surmeier, D.J., 2013. Calcium entry and α-synuclein inclusions elevate dendritic mitochondrial oxidant stress in dopaminergic neurons. J. Neurosci. 33, 10154–10164. https://doi.org/10.1523/JNEUROSCI.5311-12.2013.

Egenrieder, L., Mitricheva, E., Spanagel, R., Noori, H.R., 2020. No basal or drug-induced sex differences in striatal dopaminergic levels: a cluster and meta-analysis of rat microdialysis studies. J. Neurochem 152, 482–492. https://doi.org/10.1111/jnc.14911.

El Ayadi, A., Afailal, I., Errami, M., 2001. Effects of voltage-sensitive calcium channel blockers on extracellular dopamine levels in rat striatum. Metab. Brain Dis. 16, 121–131. https://doi.org/10.1023/a:1012549225235.

de Erausquin, G., Brooker, G., Hanbauer, I., 1992. K^+-evoked dopamine release depends on a cytosolic Ca^{2+} pool regulated by N-type Ca^{2+} channels. Neurosci. Lett. 145, 121–125. https://doi.org/10.1016/0304-3940(92)90001-N.

Eriguchi, M., Iida, K., Ikeda, S., Osoegawa, M., Nishioka, K., Hattori, N., Nagayama, H., Hara, H., 2019. Parkinsonism relating to intoxication with glyphosate. Intern Med 58, 1935–1938. https://doi.org/10.2169/internalmedicine.2028-18.

Faria, M., Bedrossiantz, J., Ramírez, J.R.R., Mayol, M., García, G.H., Bellot, M., Prats, E., Garcia-Reyero, N., Gómez-Canela, C., Gómez-Oliván, L.M., Raldúa, D., 2021. Glyphosate targets fish monoaminergic systems leading to oxidative stress and anxiety. Environ. Int 146, 106253. https://doi.org/10.1016/j.envint.2020.106253.

Faro, L.R.F., Alfonso, M., Ferreira, V.M., Durán, R., 2018. Role of voltage-gated calcium channels on striatal dopamine release induced by inorganic mercury in freely moving rats. Environ. Toxicol. Pharm. 59, 13–16. https://doi.org/10.1016/j.etap.2018.02.005.

Faro, L.R.F., Costas-Ferreira, C., Pantoja, A.A., Durán, R., 2022. Protective effects of antioxidants on striatal dopamine release induced by organophosphorus pesticides. Pest Biochem Physiol. 182, 105035 https://doi.org/10.1016/j.pestbp.2022.105035.

Furukawa, T., Yamakawa, T., Midera, T., Sagawa, T., Mori, Y., Nukada, T., 1999. Selectivities of dihydropyridine derivatives in blocking Ca2+ channel subtypes expressed in xenopusoocytes. J. Pharmacol. Exp. Ther. 291, 464–473.

Gallegos, C.E., Bartos, M., Gumilar, F., Raisman-Vozari, R., Minetti, A., Baier, C.J., 2020. Intranasal glyphosate-based herbicide administration alters the redox balance and the cholinergic system in the mouse brain. Neurotoxicology 77, 205–215. https://doi.org/10.1016/j.neuro.2020.01.007.

Geer, J.J., Dooley, D.J., Adams, M.E., 1993. K(+)-stimulated $45Ca^{2+}$ flux into rat neocortical mini-slices is blocked by omega-Aga-IVA and the dual Na^+/Ca^{2+} channel blockers lidoflazine and flunarizine. Neurosci. Lett. 158, 97–100. https://doi.org/10.1016/0304-3940(93)90621-q.

Guilbert, C., James, T.L., 2008. Docking to RNA via root-mean-square-deviation-driven energy minimization with flexible ligands and flexible targets. J. Chem. Inf. Model 48, 1257–1268. https://doi.org/10.1021/ci8000327.

Gutowska, I., Machoy, Z., Machaliński, B., 2005. The role of bivalent metals in hydroxyapatite structures as revealed by molecular modeling with the HyperChem software. J. Biomed. Mater. Res A 75, 788–793. https://doi.org/10.1002/jbm.a.30511.

Harding, E.K., Souza, I.A., Gardini, M.A., Gadotti, V.M., Ali, M.Y., Huang, S., Antunes, F. T.T., Trang, T., Zamponi, G.W., 2023. Differential regulation of $Cav_{3.2}$ and $Cav_{2.2}$ calcium channels by CB_1 receptors and cannabidiol. Br. J. Pharm. 180, 1616–1633. https://doi.org/10.1111/bph.16035.

He, L., Yu, Z., Geng, Z., Huang, Z., Zhang, C., Dong, Y., Gao, Y., Wang, Y., Chen, Q., Sun, L., Ma, X., Huang, B., Wang, X., Zhao, Y., 2022. Structure, gating, and pharmacology of human $CaV_{3.3}$ channel. Nat. Commun. 13, 1–9. https://doi.org/10.1038/s41467-022-29728-0.

Hernández-Plata, I., Giordano, M., Díaz-Muñoz, M., Rodríguez, V.M., 2015. The herbicide glyphosate causes behavioral changes and alterations in dopaminergic markers in male Sprague-Dawley rat. Neurotoxicology 46, 79–91. https://doi.org/10.1016/j.neuro.2014.12.001.

Hevener, K.E., Zhao, W., Ball, D.M., Babaoglu, K., Qi, J., White, S.W., Lee, R.E., 2009. Validation of molecular docking programs for virtual screening against dihydropteroate synthase. J. Chem. Inf. Model 49, 444–460. https://doi.org/10.1021/ci800293n.

Kato, T., Otsu, Y., Furune, Y., Yamamoto, T., 1992. Different effects of L-, N-and T-type calcium channel blockers on striatal dopamine release measured by microdialysis in freely moving rats. Neurochem. Int. 21, 99–107. https://doi.org/10.1016/0197-0186(92)90072-y.

Kimura, M., Yamanishi, Y., Hanada, T., Kagaya, T., Kuwada, M., Watanabe, T., Katayama, K., Nishizawa, Y., 1995. Involvement of P-type calcium channels in high potassium-elicited release of neurotransmitters from rat brain slices. Neuroscience 66, 609–615. https://doi.org/10.1016/0306-4522(95)00023-C.

Krebs, M.O., Trovero, F., Desban, M., Gauchy, C., Glowinski, J., Kemel, M.L., 1991. Distinct presynaptic regulation of dopamine release through NMDA receptors in striosome- and matrix-enriched areas of the rat striatum. J. Neurosci. 11, 1256–1262. https://doi.org/10.1523/JNEUROSCI.11-05-01256.1991.

Larsen, K.E., Lifschitz, A.L., Lanusse, C.E., Virkel, G.L., 2016. The herbicide glyphosate is a weak inhibitor of acetylcholinesterase in rats. Environ. Toxicol. Pharm. 45, 41–44. https://doi.org/10.1016/j.etap.2016.05.012.

Lohr, C., Heil, J.E., Deitmer, J.W., 2005. Blockage of voltage-gated calcium signaling impairs migration of glial cells in vivo. Glia, 50, 198–211. https://doi.org/10.1002/glia.20163.

Martínez, M.-A., Ares, I., Rodríguez, J.-L., Martínez, M., Martínez-Larrañaga, M.-R., Anadón, A., 2018. Neurotransmitter changes in rat brain regions following glyphosate exposure. Environ. Res 161, 212–219. https://doi.org/10.1016/j.envres.2017.10.051.

Martínez, M.-A., Rodríguez, J.-L., Lopez-Torres, B., Martínez, M., Martínez-Larrañaga, M.-R., Maximiliano, J.-E., Anadón, A., Ares, I., 2020. Use of human neuroblastoma SH-SY5Y cells to evaluate glyphosate-induced effects on oxidative stress, neuronal development and cell death signaling pathways. Environ. Int 135, 105414. https://doi.org/10.1016/j.envint.2019.105414.

Martínez-Fong, D., Rosales, M.G., Góngora-Alfaro, JoséL., Hernández, S., Aceves, G., 1992. NMDA receptor mediates dopamine release in the striatum of unanesthetized rats as measured by brain microdialysis. Brain Res. 595, 309–315. https://doi.org/10.1016/0006-8993(92)91065-M.

Meiser, J., Weindl, D., Hiller, K., 2013. Complexity of dopamine metabolism. Cell Commun. Signal 11, 34. https://doi.org/10.1186/1478-811X-11-34.

Meng, X.-Y., Zhang, H.X., Mezei, M., Cui, M., 2012. Molecular docking: a powerful approach for structure-based drug discovery. Curr. Comput. Aided-Drug Des. 7, 146–157. https://doi.org/10.2174/157340911795677602.

Monzani, E., Nicolis, S., Dell'Acqua, S., Capucciati, A., Bacchella, C., Zucca, F.A., Mosharov, E.V., Sulzer, D., Zecca, L., Casella, L., 2019. Dopamine, oxidative stress and protein–quinone modifications in Parkinson's and other neurodegenerative diseases. Angew. Chem. Int Ed. 58, 6512–6527. https://doi.org/10.1002/anie.201811122.

Nolan, S.O., Zachry, J.E., Johnson, A.R., Brady, L.J., Siciliano, C.A., Calipari, E.S., 2020. Direct dopamine terminal regulation by local striatal microcircuitry. J. Neurochem 155, 475–493. https://doi.org/10.1111/jnc.15034.

Okita, M., Watanabe, Y., Taya, K., Utsumi, H., Hayashi, T., 2000. Presynaptic L-type Ca^{2+} channels on excessive dopamine release from rat caudate putamen. Physiol. Behav. 68, 641–649. https://doi.org/10.1016/S0031-9384(99)00227-9.

Ortega-Carrasco, E., Lledós, A., Maréchal, J.D., 2014. Assessing protein-ligand docking for the binding of organometallic compounds to proteins. J. Comput. Chem. 35, 192–198. https://doi.org/10.1002/jcc.23472.

Pan, Z.H., Hu, H.J., Perring, P., Andrade, R., 2001. T-type Ca^{2+} channels mediate neurotransmitter release in retinal bipolar cells. Neuron 32, 89–98. https://doi.org/10.1016/s0896-6273(01)00454-8.

Patrick, G.L., 2013. An introduction to medicinal chemistry. Oxford University Press, United Kingdom, pp. 5–13.

Paxinos, G., Watson, C., 1998. The Rat Brain: In Stereotaxic Coordinates, fourth ed. Academic Press, New York.

Phillips, P.E., Stamford, J.A., 2000. Differential recruitment of N-, P- and Q-type voltage-operated calcium channels in striatal dopamine release evoked by "regular" and "burst" firing. Brain Res. 884, 139–146. https://doi.org/10.1016/s0006-8993(00)02958-9.

Rocchitta, G., Delogu, R.M., Migheli, R., Solinas, L., Susini, G., Desole, M.S., Miele, E., Miele, M., Serra, P.A., 2004. On the mechanism of levosimendan-induced dopamine release in the striatum of freely moving rats. J. Pharmacol. Sci. 95, 299–304. https://doi.org/10.1254/jphs.fpe04003x.

Rusakov, D.A., 2006. Ca^{2+}-dependent mechanisms of presynaptic control at central synapses. Neuroscientist 12, 317–326. https://doi.org/10.1177/1073858405284672.

Sobjak, T.M., Romão, S., do Nascimento, C.Z., dos Santos, A.F.P., Vogel, L., Guimarães, A.T.B., 2017. Assessment of the oxidative and neurotoxic effects of glyphosate pesticide on the larvae of Rhamdia quelen fish. Chemosphere 182, 267–275. https://doi.org/10.1016/j.chemosphere.2017.05.031.

Takada, M., Kang, Y., Imanishi, M., 2001. Immunohistochemical localization of voltage-gated calcium channels in substantia nigra dopamine neurons. Eur. J. Neurosci. 13, 757–762. https://doi.org/10.1046/j.1460-9568.2001.01435.x.

Tang, A.-H., Karson, M.A., Nagode, D.A., McIntosh, J.M., Uebele, V.N., Renger, J.J., Klugmann, M., Milner, T.A., Alger, B.E., 2011. Nerve terminal nicotinic acetylcholine receptors initiate quantal GABA release from perisomatic interneurons by activating axonal T-type (Cav_3) Ca^{2+} channels and Ca^{2+} release from stores. J. Neurosci. 31, 13546–13561. https://doi.org/10.1523/JNEUROSCI.2781-11.2011.

Thaler, C., Li, W., Brehm, P., 2001. Calcium channel isoforms underlying synaptic transmission at embryonic Xenopus neuromuscular junctions. J. Neurosci. 21, 412–422. https://doi.org/10.1523/JNEUROSCI.21-02-00412.2001.

Tippens, A.L., Pare, J.-F., Langwieser, N., Moosmang, S., Milner, T.A., Smith, Y., Lee, A., 2008. Ultrastructural evidence for pre- and postsynaptic localization of $Cav_{1.2}$ L-type Ca^{2+} channels in the rat hippocampus. J. Comp. Neurol. 506, 569–583. https://doi.org/10.1002/cne.21567.

Turner, T.J., 2004. Nicotine enhancement of dopamine release by a calcium-dependent increase in the size of the readily releasable pool of synaptic vesicles. J. Neurosci. 24, 11328–11336. https://doi.org/10.1523/JNEUROSCI.1559-04.2004.

Turner, T.J., Adams, M.E., Dunlap, K., 1993. Multiple Ca^{2+} channel types coexist to regulate synaptosomal neurotransmitter release. Proc. Natl. Acad. Sci. USA 90, 9518–9522.

Verdonk, M.L., Cole, J.C., Hartshorn, M.J., Murray, C.W., Taylor, R.D., 2003. Improved protein-ligand docking using GOLD. Proteins 52, 609–623. https://doi.org/10.1002/prot.10465.

Weiss, N., Hameed, S., Fernández-Fernández, J.M., Fablet, K., Karmazinova, M., Poillot, C., Proft, J., Chen, L., Bidaud, I., Monteil, A., Huc-Brandt, S., Lacinova, L., Lory, P., Zamponi, G.W., De Waard, M., 2012. A $Cav_{3.2}$/syntaxin-1A signaling complex controls T-type channel activity and low-threshold exocytosis. J. Biol. Chem. 287, 2810–2818. https://doi.org/10.1074/jbc.M111.290882.

Yao, X., Gao, S., Yan, N., 2022. Structural basis for pore blockade of human voltage-gated calcium channel $Cav_{1.3}$ by motion sickness drug cinnarizine. Cell Res. 32, 946–948. https://doi.org/10.1038/s41422-022-00663-5.

Ye, Q., Yan, L.Y., Xue, L.J., Wang, Q., Zhou, Z.K., Xiao, H., Wan, Q., 2011. Flunarizine blocks voltage-gated Na+ and Ca2+ currents in cultured rat cortical neurons: a possible locus of action in the prevention of migraine. Neurosci. Lett. 487, 394–399. https://doi.org/10.1016/j.neulet.2010.10.064.

Yin, Y., Zhang, G., Xu, X., Zhao, P., Ma, L., 2021. Intermolecular hydrogen bond ruptured by graphite with different lamellar number. R. Soc. Open Sci. 8, 210565 https://doi.org/10.5061/dryad.9cnp5hqjh.

Zamponi, G.W., Striessnig, J., Koschak, A., Dolphin, A.C., 2015. The physiology, pathology, and pharmacology of voltage-gated calcium channels and their future therapeutic potential. Pharm. Rev. 67, 821–870. https://doi.org/10.1124/pr.114.009654.

Zheng, Q., Yin, J., Zhu, L., Jiao, L., Xu, Z., 2018. Reversible Parkinsonism induced by acute exposure glyphosate. Park. Relat. Disord. 50, 121. https://doi.org/10.1016/j.parkreldis.2018.01.021.